Electronic Supplementary Information

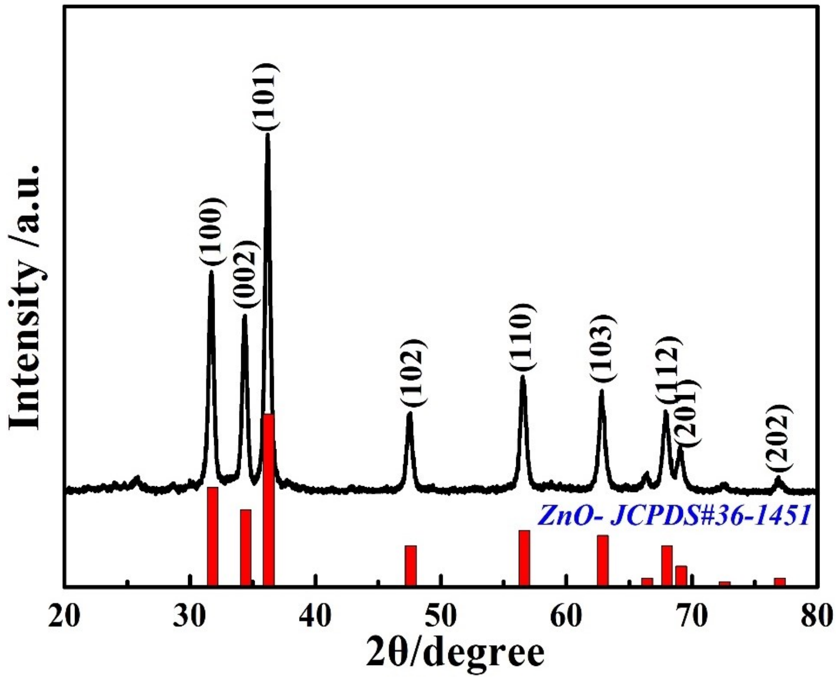

Fig. S1 XRD pattern of ZnO microflowers.

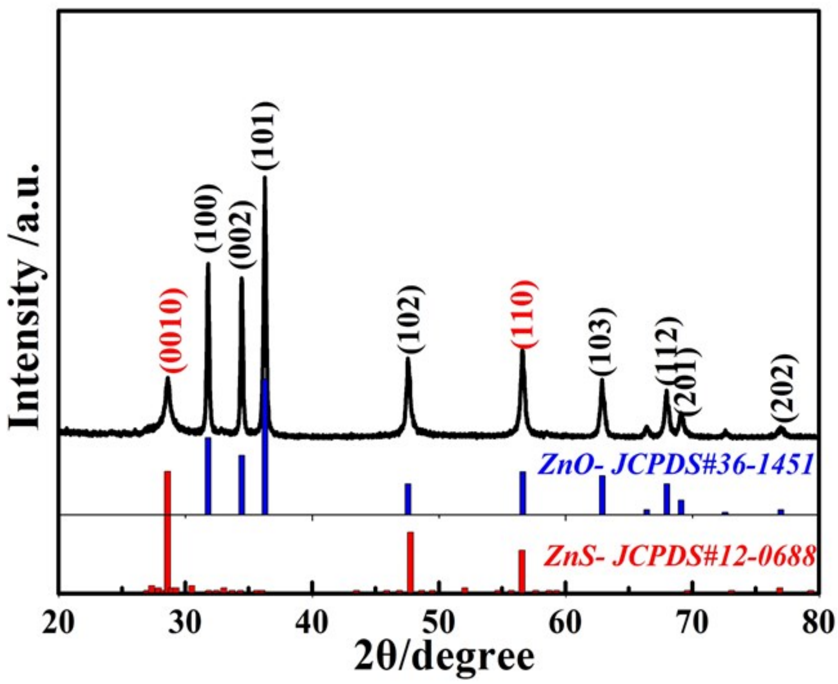

Fig. S2 XRD pattern of ZnO/ZnS microflowers.

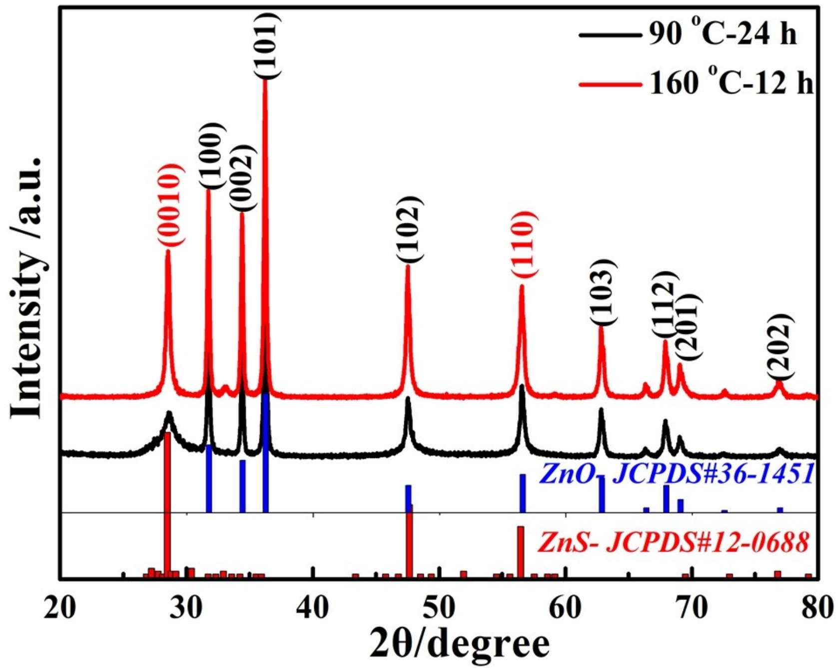

Fig. S3 XRD pattern of ZnO/ZnS microflowers by directly vulcanizing ZnO template at different reaction time and reaction temperature.

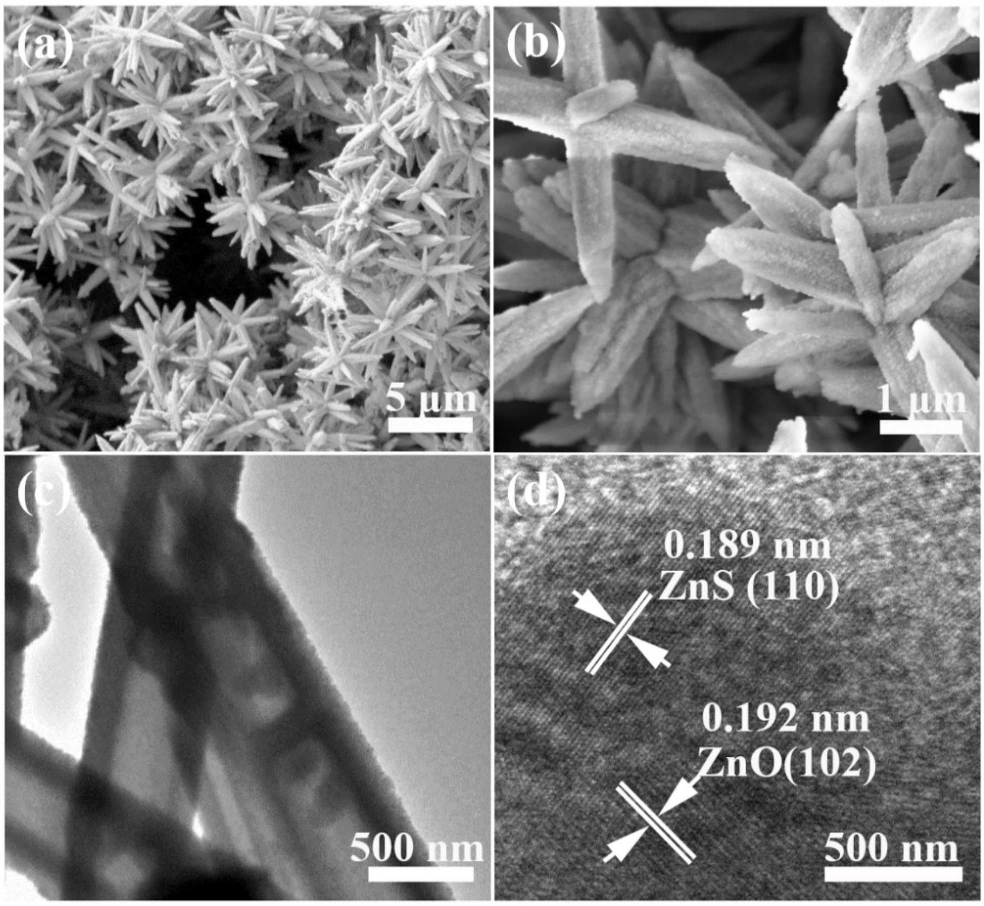

Fig. S4 Morphology characterization of hollow ZnO/ZnS microflowers: (a, b) SEM, (c) TEM, and (d) HRTEM images.

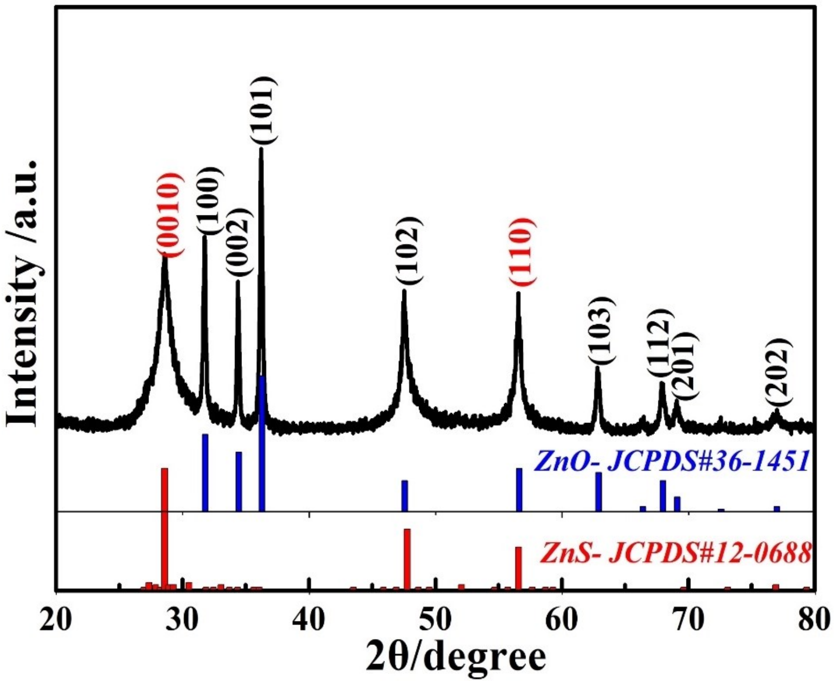

Fig. S5 XRD pattern of hollow ZnO/ZnS@C microflowers.

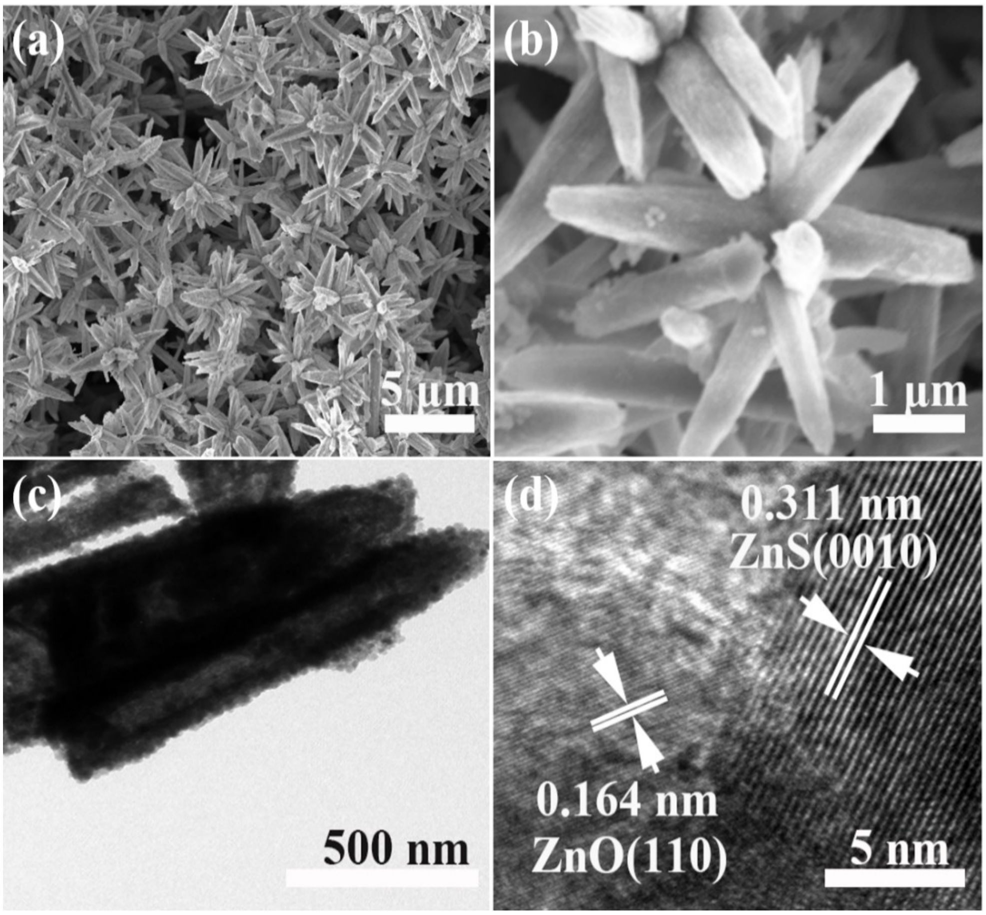

Fig. S6 Morphology characterization of hollow ZnO/ZnS@C microflowers: (a, b) SEM, (c) TEM, and (d) HRTEM images.

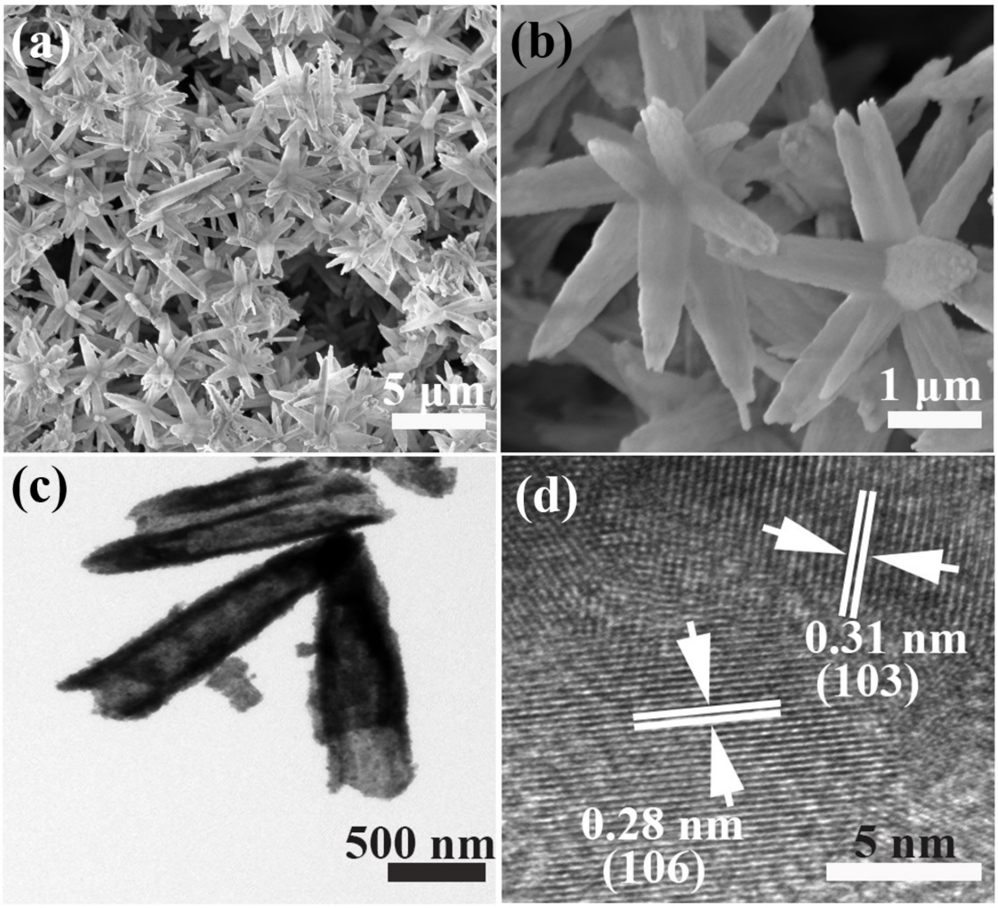

Fig. S7 Morphology characterization of the hollow ZnS@C microflowers: (a, b) SEM (c) TEM, and (d) HRTEM images.

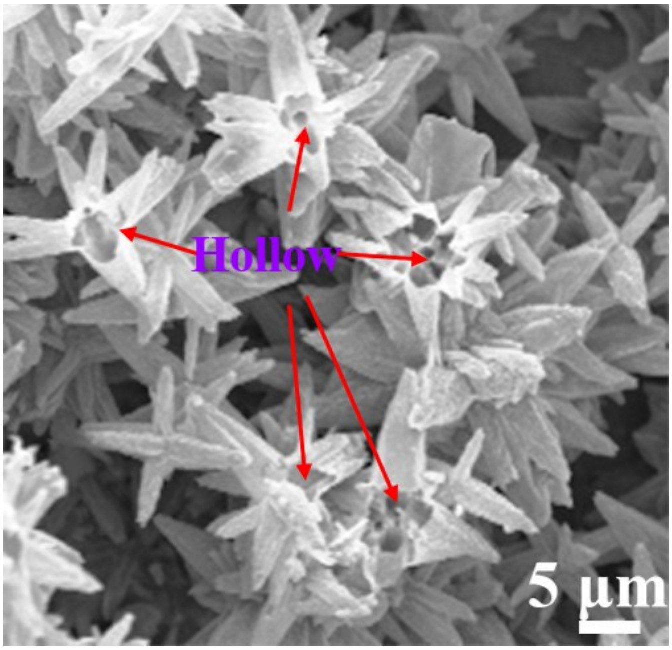

Fig. S8 SEM image of ZnS/CuS@C microflowers with hollow structure.

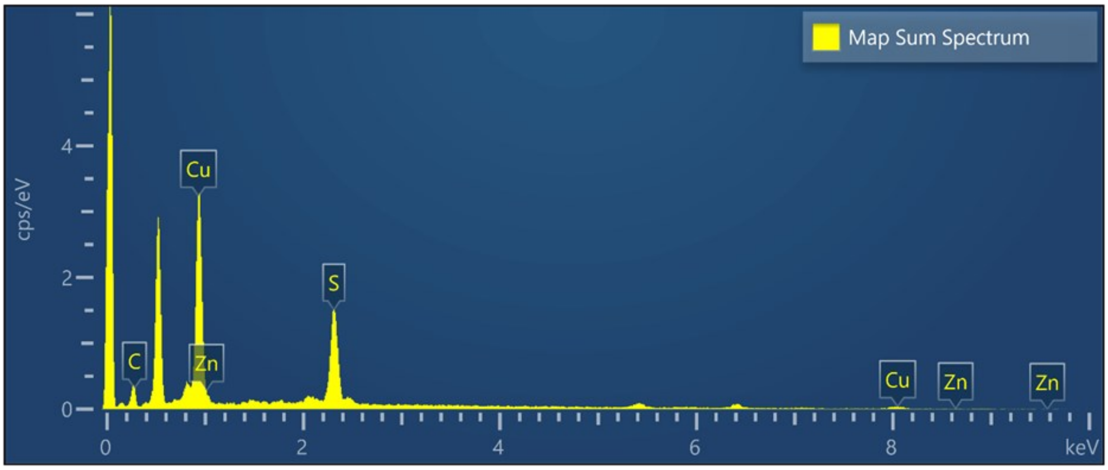

Fig. S9 EDS spectrum of hollow ZnS/CuS@C microflowers.

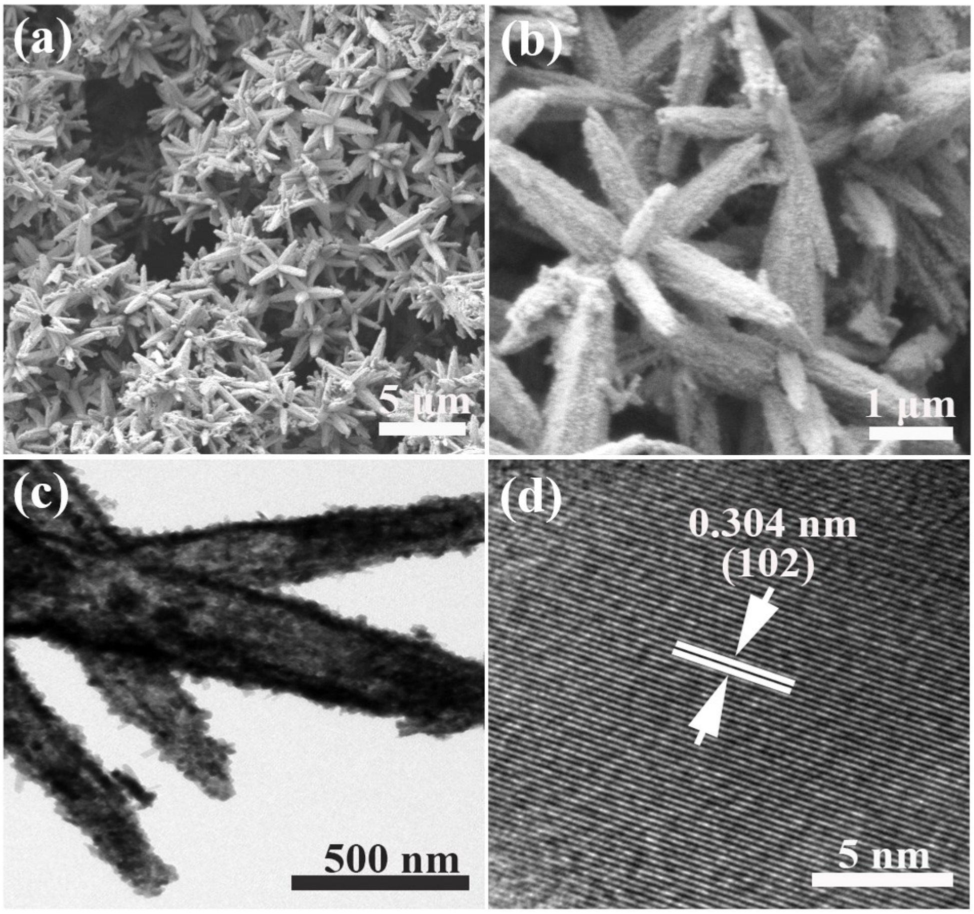

Fig. S10 Morphology characterization of hollow CuS@C microflowers: (a, b) SEM, (c) TEM, and (d) HRTEM images.

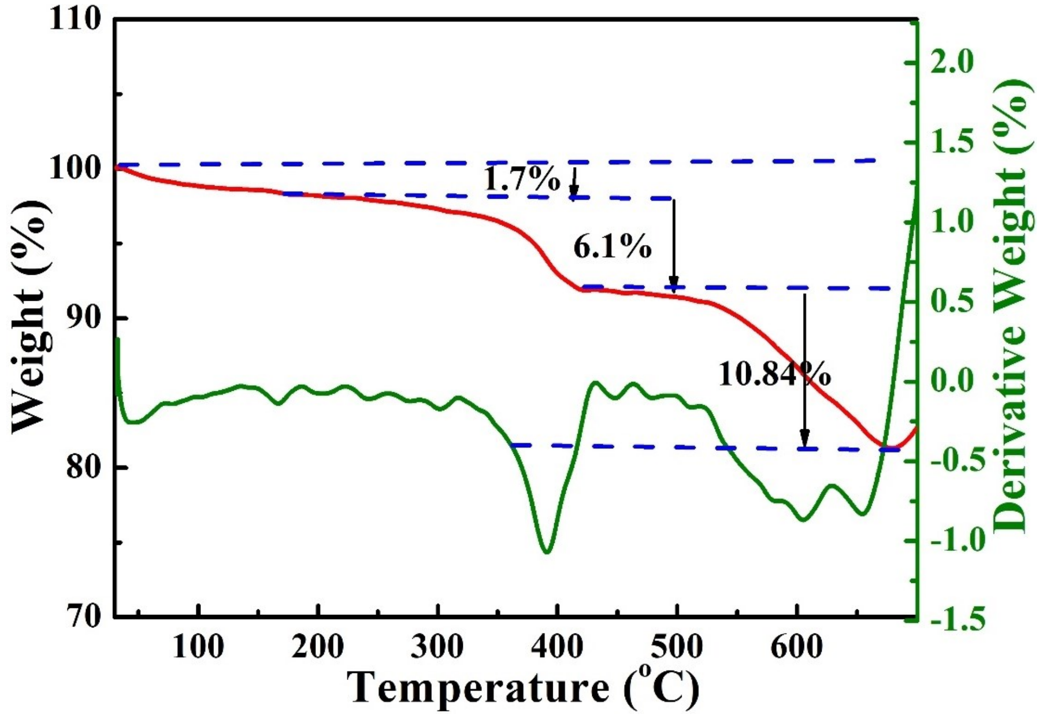

Fig. S11 TGA curve of hollow ZnS/CuS@C microflowers.

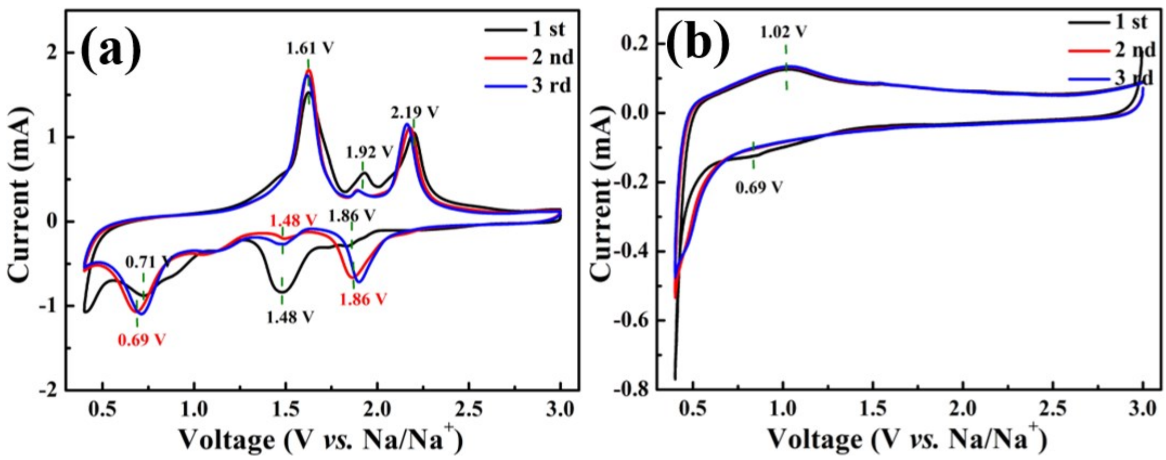

Fig. S12 CV curves of CuS@C (a) and ZnS@C (b) electrodes at a sweep rate of 0.5 mV s^{-1}.

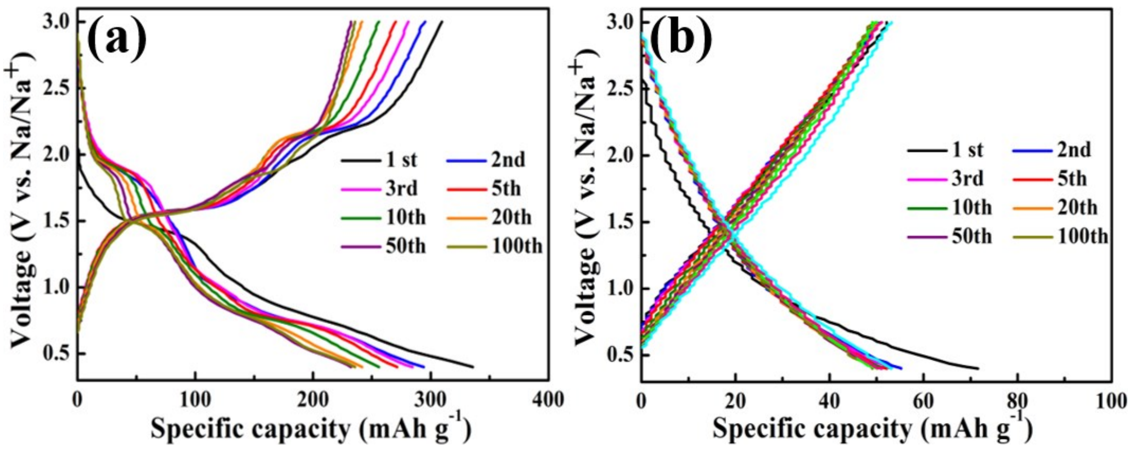

Fig. S13 Galvanostatic discharge–charge curves of CuS@C (a) and ZnS@C (b) electrodes at 2 A g^{-1}.

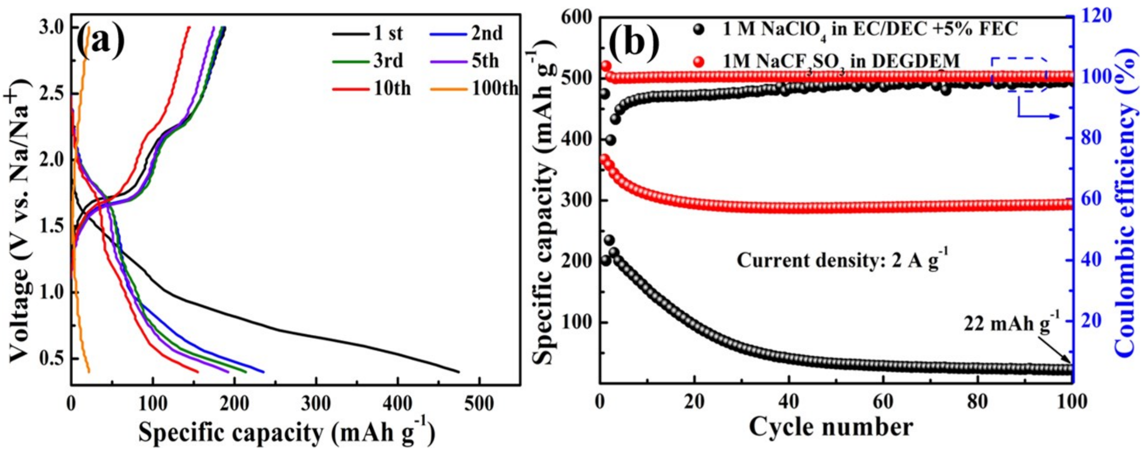

Fig. S14 (a) Galvanostatic discharge–charge curves of ZnS/CuS@C electrode at 2 A g^{-1} using 1 M $NaClO_4$ in EC/DEC with 5% FEC. (b) Comparison of cycling stability of ZnS/CuS@C electrode at different electrolytes.

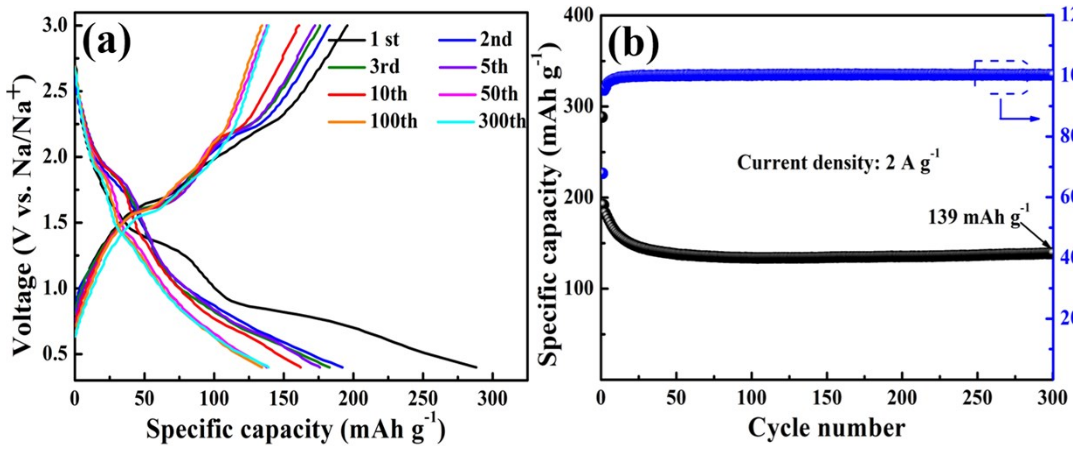

Fig. S15 Galvanostatic discharge–charge curves (a) and cycling performance (b) of the mixture ZnS@C and CuS@C with a weight ratio of 1:1.

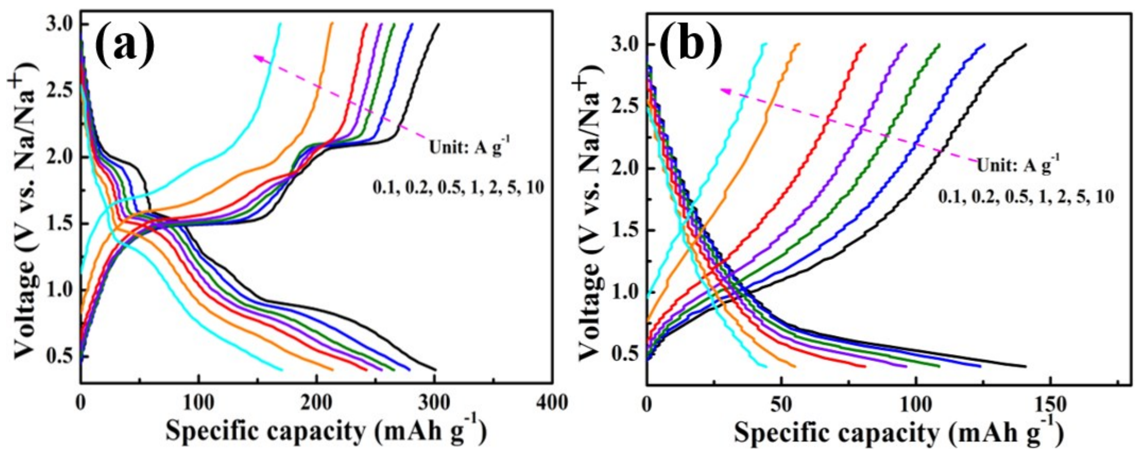

Fig. S16 Discharge–charge curves of CuS@C (a) and ZnS@C (b) electrodes at different current rates.

Table S1 A comparison of cycling performance and specific capacity about ZnS, ZnSe, and CuS-based SIBs anode.

Materials	Voltage window (V)	Rate (A g^{-1})	Cycle number	Capacity (mAh g^{-1})	Ref.
Sb/ZnS@C	0.1-1.8	0.1	150	613.0	1
ZnS/Fe_9S_{10}	0.005-3.0	1.0	200	485.0	2
ZnS/SnS_2	0.1-3.0	5.0	700	456.2	3
$ZnSe/Sb_2Se_3$	0.01-3.0	5.0	250	295.0	4
$SnSe_2$/ZnSe@PDA	0.1-3.0	1.0	1000	616.0	5
Fe_7S_8/C@ZnS/N-C@C	0.01-3.0	5.0	10000	364.7	6
ZnS-Sb_2S_3@C	0.01-1.8	0.1	120	630.0	7
ZnSe-NC@$CoSe_2$-NC	0.005-3.0	0.1	150	308.5	8
ZnSe/$MoSe_2$@C	0.01-3.0	4.0	600	524.0	9
ZnS/Co_3S_4	0.01-3.0	1.0	200	750.0	10
SnS/ZnS@C	0.01-3.0	0.2	250	485.0	11
CuS@CoS_2	0.4-2.6	0.5	500	410.0	12
WS_{2-x} @ZnS @C	0.01-3.0	5.0	5000	170.8	13
ZnS/CuS@C	**0.4-3.0**	**5.0**	**1330**	**342.0**	**This work**
		10.0	**1750**	**282.7**	

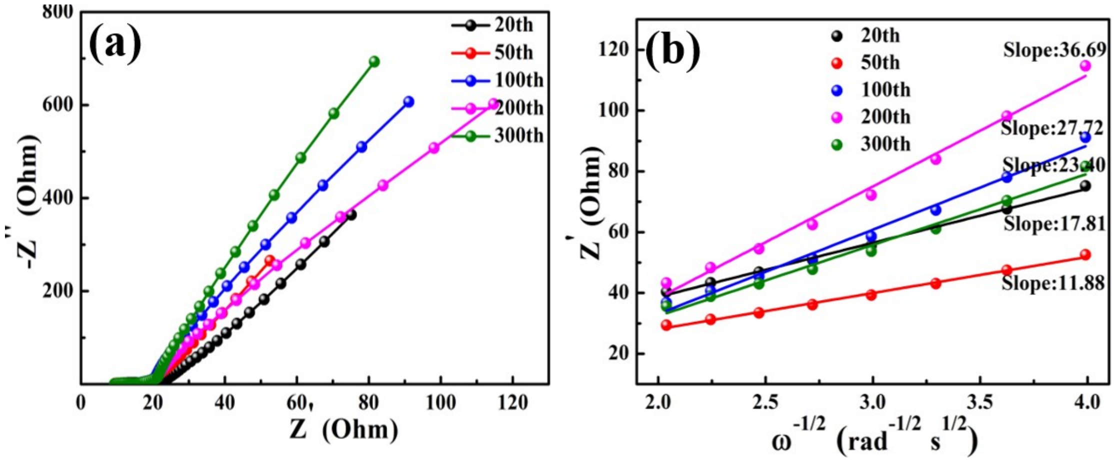

Fig. S17 Nyquist plots (a) and the linear relationships between Z′ and $\omega^{-1/2}$ (b) of ZnS/CuS@C electrode at different cycles.

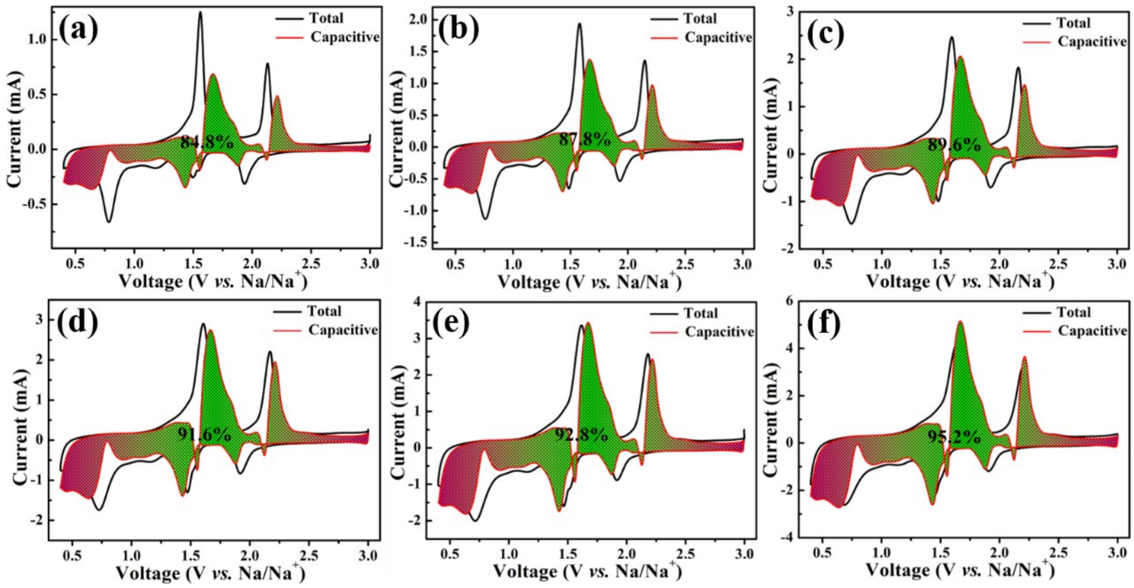

Fig. S18 CV curves and the capacitive contribution represented by the colours region at different scan rates: (a) 0.2 mV s^{-1}; (a) 0.4 mV s^{-1}; (b) 0.6 mV s^{-1}; (c) 0.8 mV s^{-1}; (d) 1.0 mV s^{-1}; (e) 1.5 mV s^{-1}.

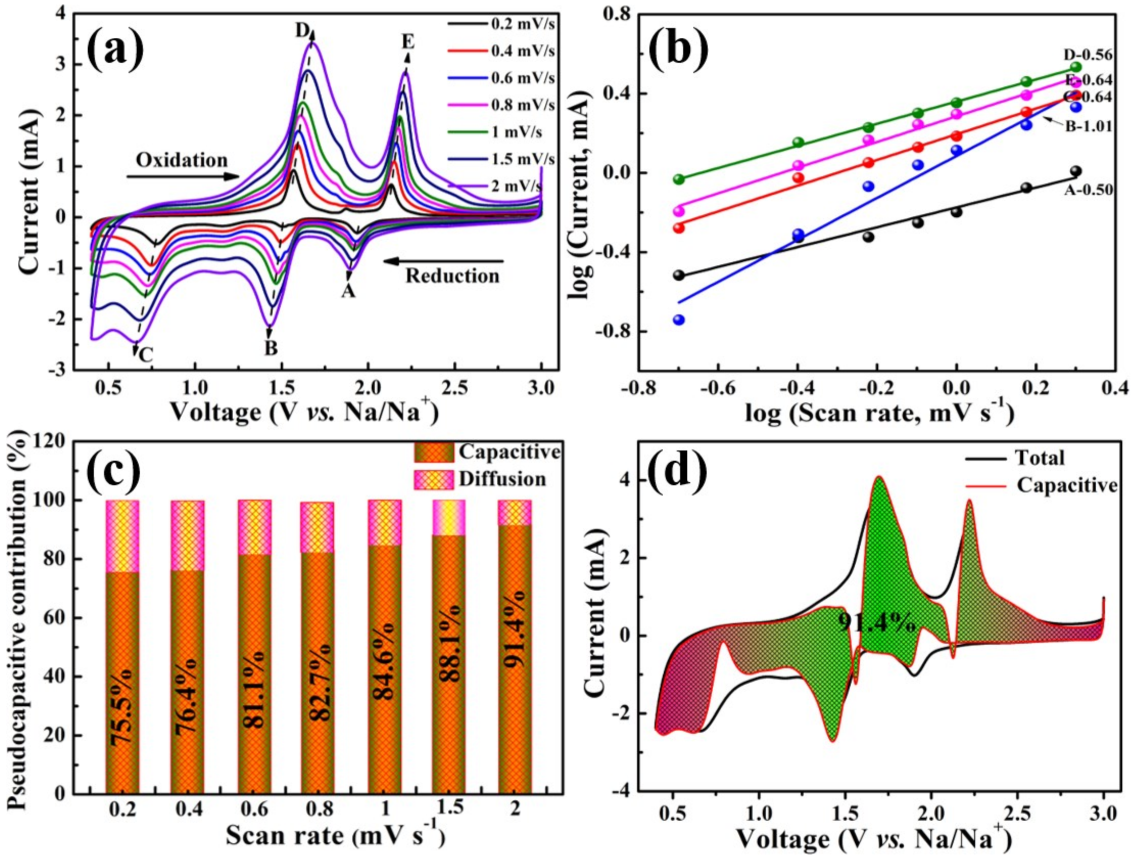

Fig. S19 (a) CV curves at different current rates from the ranges of 0.2 to 2.0 mV s^{-1}. (b) corresponding log *i* versus log *v* plots at five specific peaks. The proportions of capacitive contribution at various rates (c) and the percentage of capacitive contribution to charge storage at 2.0 mV s^{-1} (d) for CuS@C electrode.

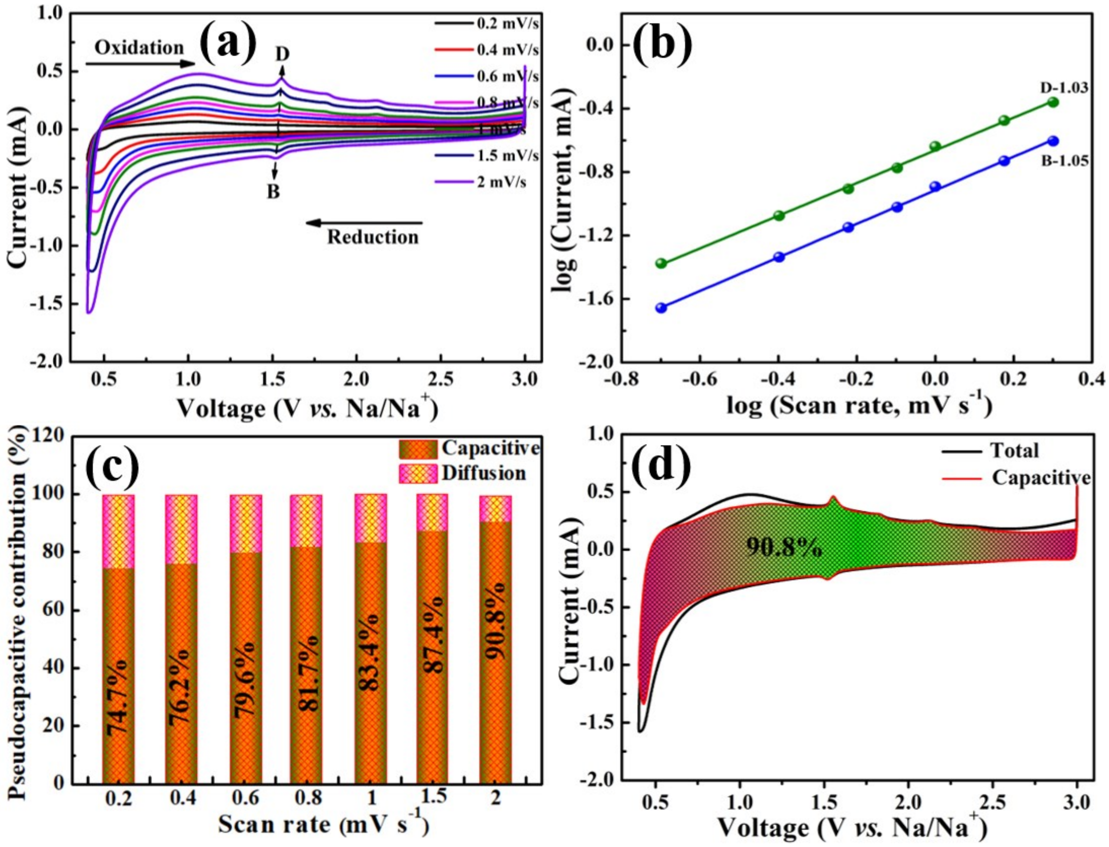

Fig. S20 (a) CV curves at different current rates from the ranges of 0.2 to 2.0 mV s^{-1}. (b) corresponding log *i* versus log *v* plots at two specific peaks. The proportions of capacitive contribution at various rates (c) and the percentage of capacitive contribution to charge storage at 2.0 mV s^{-1} (d) for ZnS@C electrode.

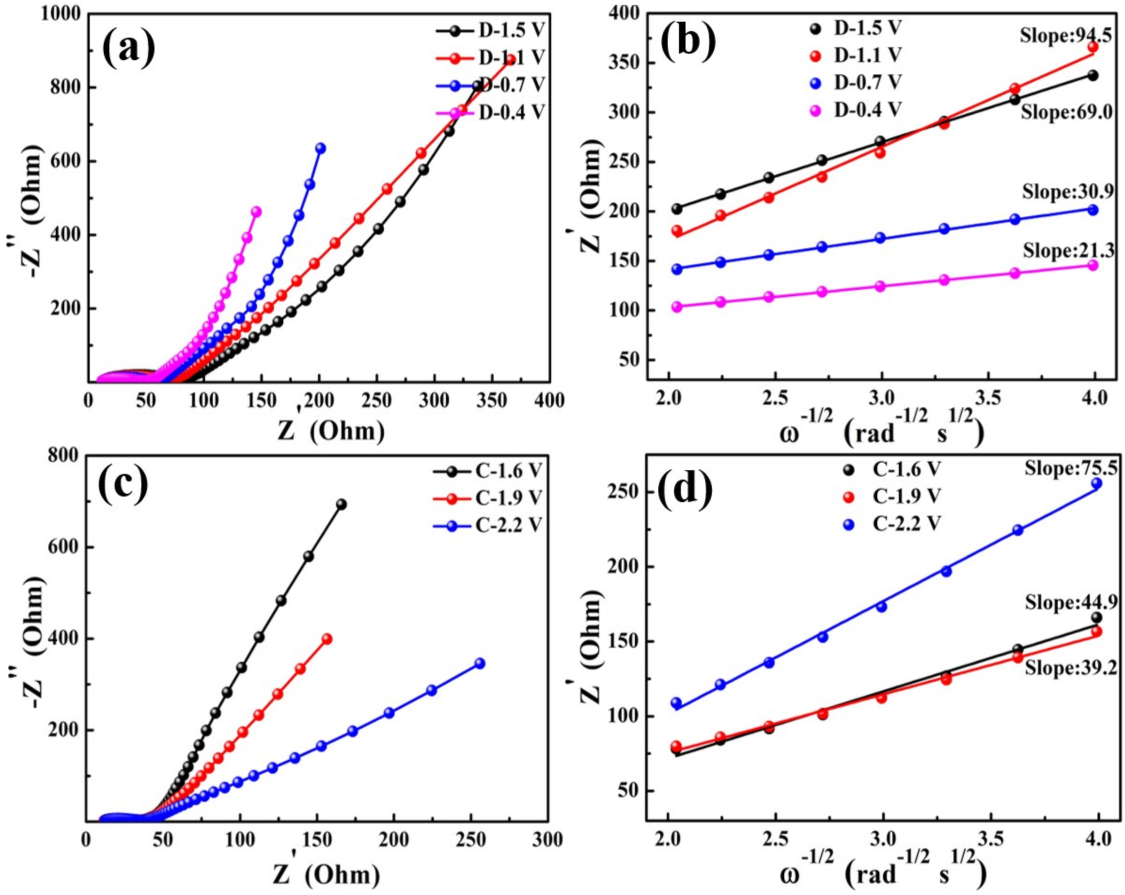

Fig. S21 Nyquist plots of ZnS/CuS@C electrode at different discharged (a) and charged (c) states. The linear relationships between Z′ and $\omega^{-1/2}$ of ZnS/CuS@C electrode at different discharged (b) and charged (d) states.

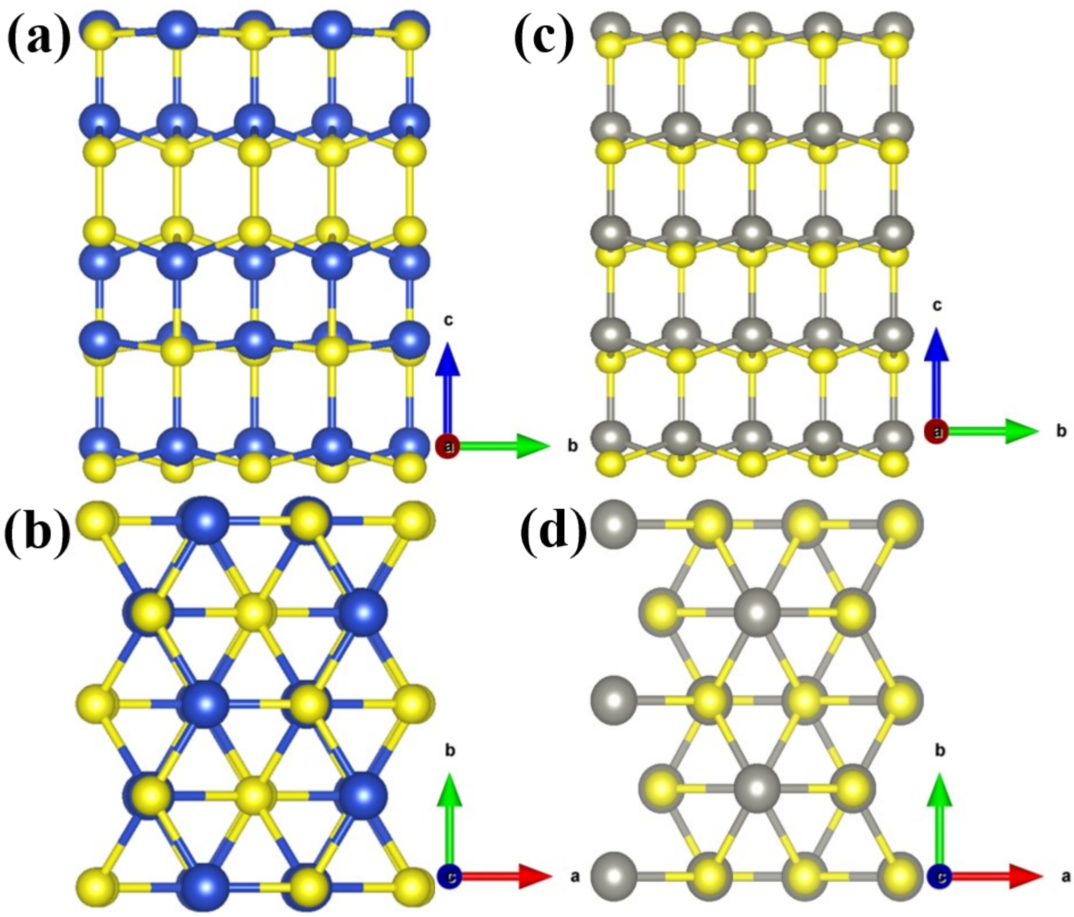

Fig. S22 Crystal structure of CuS from side (a), and plan (b) views. Crystal structure of ZnS from side (c), and plan (d) views.

References

1 S. H. Dong, C. X. Li, Z. Q. Li, L. Y. Zhang and L. W. Yin, *Small*, 2018, **14**, 1704517.

2 C. Z. Zhang, F. Han, J. M. Ma, Z. Li, F. Q. Zhang, S. H. Xu, H. B. Liu, X. K. Li, J. S. Liu and A. H. Lu, *J. Mater. Chem. A*, 2019, **7**, 11771–11781.

3 L. Cao, B. Zhang, X. Ou, C. H. Wang, C. L. Peng and J. F. Zhang, *Small*, 2019, **15**, 1804861

4 Y. Y. Wang, D. X. Cao, K. L. Zhang, W. P. Kang, X. T. Wang, P. Ma, Y. F. Wan, D. W. Cao and D. F. Sun, *Nanoscale*, 2020, **12**, 17915–17924.

5 P. Liu, J. Han, K. J. Zhu, Z. H. Dong and L. F. Jiao, *Adv. Energy Mater.*, 2020, **10**, 2000741.

6 D. W. Cao, W. P. Kang, W. H. Wang, K. A. Sun, Y. Y. Wang, P. Ma and D. F. Sun, *Small*, 2020, **16**, 1907641.

7 S. H. Dong, C. X. Li, X. L. Ge, Z. Q. Li, X. G. Miao and L. W. Yin, *ACS Nano*, 2017, **11**, 6474−6482.

8 X. J. Hu, X. J. Liu, K. Chen, G. Wang and H. Wang, *J. Mater. Chem. A*, 2019, **7**, 11016–11037.

9 L. X. Zeng, Y. X. Fang, L. H. Xu, C. Zheng, M. Q. Yang, J. F. He, H. Xue, Q. R. Qian, M. D. Wei and Q. H. Chen, *Nanoscale*, 2019, **11**, 6766–6775.

10 Z. Zhang, Y. Huang, X. D. Liu, C. Chen, Z. P. Xu and P. B. Liu, *Carbon*, 2020, **157**, 244–254.

11 J. J. Ai, X. Y. Zhao, Y. K. Lei, S. A. Yang, Q. J. Xu, C. Y. Lai and C. X. Peng, *Appl. Surf. Sci.*, 2019, **496**, 143631.

12 Y. J. Fang, B. Y. Guan, D. Y. Luan and X. W. Lou, *Angew. Chem.*, 2019, **131**, 7821–7825.

13 Y. Li, J. Qian, M. H. Zhang, S. Wang, Z. H. Wang, M. S. Li, Y. Bai, Q. Y. An, H. J. Xu, F. Wu, L. Q. Mai and C. A. Wu, *Adv. Mater.*, 2020, **32**, 2005802.